THE BELL SYSTEM TECHNICAL JOURNAL
Vol. 58, No. 5, May–June 1979
Printed in U.S.A.

A New Selective Fading Model: Application to Propagation Data

By W. D. RUMMLER

(Manuscript received September 21, 1978)

Channel transmission models for use in estimating the performance of radio systems on line-of-sight paths at 6 GHz are explored. The basis for this study is the simple three-ray multipath fade, which provides a channel transfer function of the form $H(\omega) = a[1 - b \exp -j(\omega - \omega_0)\tau]$, *where a is the scale parameter, b is a shape parameter,* τ *is the delay difference in the channel, and* ω_0 *is the (radian) frequency of the fade minimum. This model is indistinguishable from an ideal channel model, within the accuracy of existing measurements. The propagation data that confirm the model were obtained in summer 1977 from a 26.4-mile hop near Atlanta, Georgia. The received power at 24 sample frequencies spaced at 1.1 MHz and centered on 6034.2 MHz was continuously monitored and recorded during periods of anomalous behavior. The model is applied to estimating the statistics of the channel delay difference,* τ. *The average delay difference giving rise to significant selectivity in the channel is between 5 and 9 ns. The distribution of delay difference is obtained for delay differences greater than 10 ns. The channel is found to have more than 3 dB of selectivity (difference between maximum and minimum attenuation in band) due to delay differences greater than 20 ns for more than 70 seconds in a heavy fading month. (This is comparable to the time the channel attenuation of a single frequency exceeds 40 dB.) The three-path model requires further simplification for narrowband channel application. For a channel with 30 MHz bandwidth, a model with fixed delay of 6.3 ns provides a sufficiently accurate representation of all observed channel conditions. The resulting nonphysical model is used to statistically characterize the condition of the fading channel. The statistics of the parameters of the fixed delay model are almost independent and of relatively simple form. The distribution of the shape parameter b is of the form* $(1 - b)^{2.3}$. *The distribution of a is lognormal. For* $b > 0.5$, *the mean and standard deviation of* -20 *(log a) are 25 and 5 dB, respectively; the*

mean decreases to 15 dB for smaller values of b. The probability density function of ω_0 is uniform at two levels; measuring ω_0 from the center of the band, the magnitude of $\omega_0\tau$ is five times as likely to be less than $\pi/2$ than to be greater. A companion paper describes the use of this model for determining the bit error rate statistics of a digital radio system on the modeled path.

I. INTRODUCTION

Performance prediction of a digital radio system on a line-of-sight microwave channel requires an accurate statistical model of the channel. Because different digital radio systems may have different sensitivities to the various channel impairments, the model must be complete to the extent that it must be capable of duplicating the amplitude and phase (at least approximately) of all observed channel conditions. To facilitate laboratory measurements and computer simulations for calculating outage, the model should be realizable as a practical test circuit and should have as few parameters as possible. Most important, the parameters should be statistically well behaved.

Two types of models have been generally considered for line-of-sight microwave radio channels: power series type models[1-3] and multipath models.[4-6] A power series model will require a few terms only if the channel is a multipath medium with a small spread of delays relative to the reciprocal bandwidth of the channel.[3] This implies that one must understand the channel as a multipath medium to understand the behavior of a power series model. Hence, we have limited our characterization efforts to multipath models.

The basis for this study is the simple three-ray multipath fade.[7] If the fading in a channel can be characterized by a simple three-path model, the channel will (as shown in Section II) have a voltage transfer function of the form

$$H(\omega) = a[1 - be^{\pm j(\omega-\omega_0)\tau}]. \tag{1}$$

where the real positive parameters a and b control the scale and shape of the fade, respectively, τ is the delay difference in the channel, and ω_0 is the radian frequency of the fade minimum. The plus and minus signs in the exponent correspond, respectively, to the channel being in a nonminimum phase or minimum phase state. Note that, with appropriate choices of parameters, this model can be reduced to a two-path model or a scaled two-path model, etc.

It has been shown previously,[7] and is illustrated in Section II, that the simple three-path fade overspecifies the channel transfer function if the delay is less than ⅙ B, where B is the observation bandwidth. The critical value of τ for a 30-MHz channel is about 5.5 ns, which is comparable to the mean delay in the channel. As a consequence, unless

the channel response can be determined to an accuracy on the order of 0.001 dB, a unique set of parameters a, b, τ, and f_o cannot be determined for more than half the faded channel conditions encountered. To avoid this problem, one must suppress or fix one of the model parameters. Section II shows that the delay, τ, is the only parameter which, when fixed, produces a reasonable model.

While a model with a fixed delay may appear to be a strange choice, it has all the required characteristics for modeling the channel transfer function. Figure 1 shows the amplitude of the channel transfer function of eq. (1) on a power scale and on a decibel scale for $\tau = 6.31$ ns. With τ fixed, the response minimum is shifted with respect to frequency by varying f_o. Varying a changes the overall level and b changes the

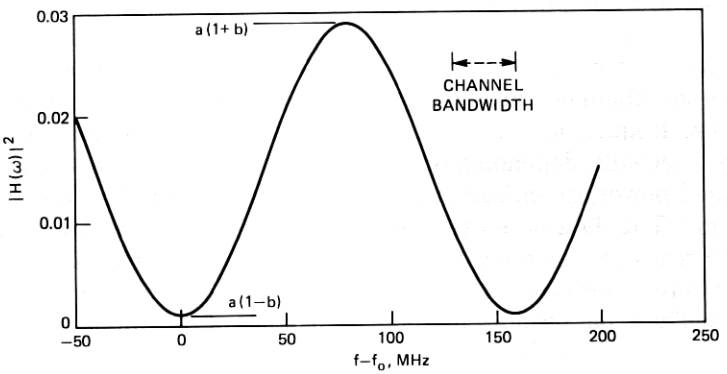

(a) MODEL POWER RATIO

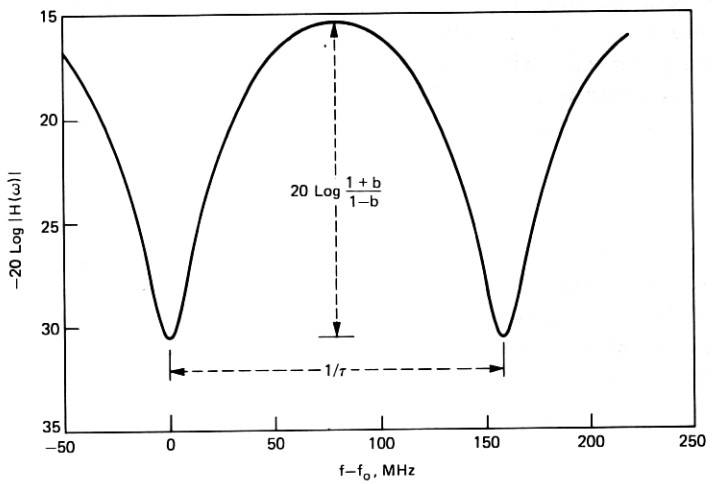

(b) MODEL ATTENUATION IN DECIBELS

Fig. 1—Channel model function. $H(\omega) = a[1 - b \exp(-j\,2\,\pi(f - f_o)\tau)]$, for $\tau = 6.3$ ns, $a = 0.1$, $b = 0.7$.

"shapeliness." If the minimum is within the 30-MHz bandwidth of a channel, the fixed delay model can generate notches with a wide range of levels and notch widths. With the minimum out of band, it can generate a wide range of combinations of levels, slopes, and curvatures within the channel bandwidth. Section VI shows that the model versatility, with τ chosen to be 6.31 ns, is sufficient to characterize a 30-MHz channel in the 6-GHz common carrier band.

Section II provides a brief discussion of the simple three-path fade. A comparative discussion of the relative merits of the different possible simplifications of this model leads to the choice of the fixed delay model.

The data used for detailed evaluation of models were obtained from a 6-GHz experiment in Palmetto, Georgia, in June 1977. The radio channel was equipped with a general trade 78-Mbit/s, 8-PSK digital radio system, and the received spectrum was monitored with a set of 24 filters with bandwidths of 200 kHz spaced at a 1.1-MHz separation across this channel. During fading activity, the received power of each of these frequencies was measured five times each second, or once every 2 seconds, depending on how rapidly the channel was changing; sampled power, quantized in 1-dB steps, was recorded by the MIDAS system.* The data base used for this study consists of approximately 25,000 scans representing 8400 seconds of fading activity; about 8700 scans were recorded during periods when the equipment was indicating errors. These data represent about 60 percent of the fading activity of a heavy fading month; therefore, the derived statistics must be viewed as provisional and subject to some modification as additional data are processed. At the very least, the data base is sufficiently large to indicate what can happen on the channel and to form a basis for choosing and validating a model.

As described in Section III, the model parameters were estimated for each scan by fitting the magnitude squared of the transfer characteristic [eq. (1)] to the observed channel shape as characterized by the power received at the sampling frequencies. Phase is subsequently derived by assuming the channel is minimum phase. Problems are encountered in realizing a minimum-phase solution because of quantization noise and the presence of certain channel shapes caused by large delays. The procedure for handling these difficulties is described.

The statistics of the parameters of the fixed delay model are discussed in Section IV. Equations providing an idealized description of the statistics of the parameters of the model are also given here.

In Section V, the determination of the delay difference present in the channel is considered. In the first subsection, it is demonstrated

* Multiple Input Data Acquisition System, constructed by G. A. Zimmerman; see Ref. 1.

that, during the observed period of fading activity, the average delay is 9 ns. A lower bound on the distribution of delay difference for large delays is developed in the second subsection. A third subsection provides an example of a channel scan that can best be approximated by a three-path fade with a delay difference of 26 ns. Fades with at least this delay and with a more moderate amount of shape (2 dB or more) were encountered for about 60 seconds of the data base studied. Thus, one might expect 26-ns delays to be present during about 100 seconds of a heavy fading month.

The presence of such large apparent delays raises questions as to the accuracy with which the fixed delay model represents the channel. These questions are addressed in Section VI where the statistics of the errors in modeling scan fits are described. The errors are small and do not compromise the usefulness of the model.

Results and conclusions are briefly summarized in Section VII.

II. CHOICE OF MODEL

In this section, we provide a brief description of the simple three-path model and show why it cannot be used to estimate delays when the delay bandwidth product is less than ⅙. In a comparative discussion, we show why the fixed delay model is the only simplification of the model that is manageable.

2.1 Simple three-path model

Consider a channel characterized by three paths or rays. The amplitude of the signal on each of these three paths, as seen by the receiver, is 1, a_1, and a_2. The second and third paths are delayed with respect to the first by τ_1 and τ_2 seconds, respectively, where $\tau_2 > \tau_1$. We define the simple three-path model by requiring the delay between the first two paths to be sufficiently small, i.e.,

$$(\omega_2 - \omega_1)\tau_1 \ll 1, \tag{2}$$

where ω_2 and ω_1 are the highest and lowest (radian) frequencies in the band. The complex voltage transfer function of the channel at a frequency ω may be illustrated with a phasor diagram. Figure 2a shows the phasor diagrams for ω_1 and ω_2 superimposed. By designating the amplitude of the (vector) sum of the first two paths by a; the angle of the sum by $\phi = \omega_0\tau - \pi$, where τ is equal to τ_2, the delay difference in the channel; and the amplitude of the third ray by ab, we obtain the simplified diagram in Fig 2b.*

* Note that, if the third amplitude is greater than the sum of the first two, we interchange the assignments of amplitudes a and ab and obtain a nonminimum phase fade.

The simple three-path fade cannot be used for a channel model because the path parameters lack uniqueness. The basic difficulty is illustrated by the two superimposed fades in Fig. 3. Note that the amplitudes of the transfer functions of these two fades match, at

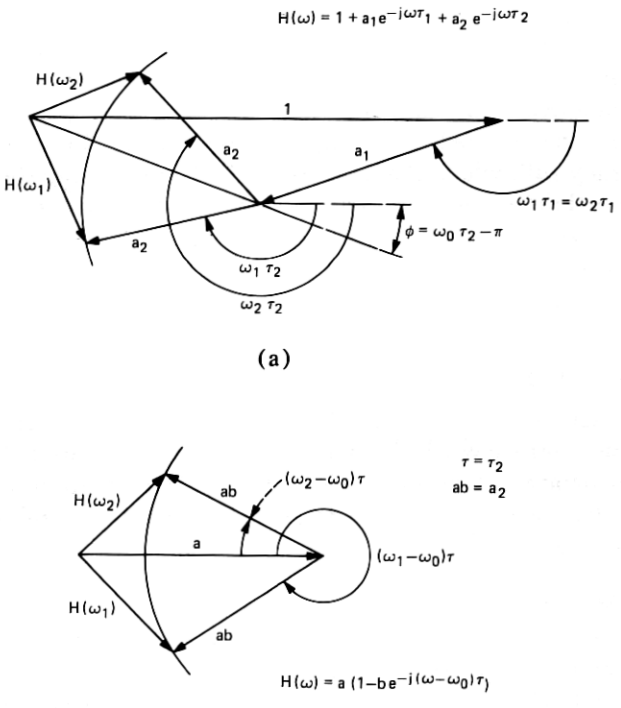

Fig. 2—Simple three-path fade. (a) Three rays shown. (b) Simplified.

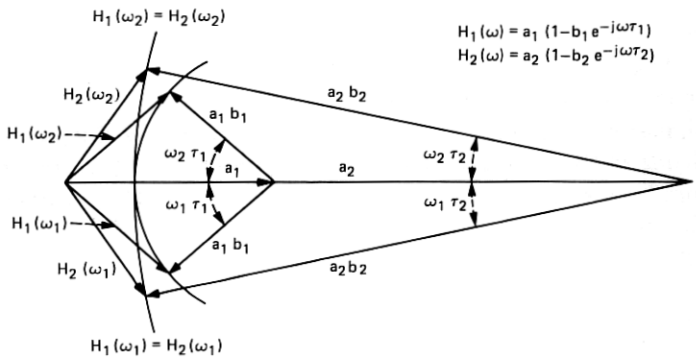

Fig. 3—Two degenerate simple three-path fades with $\omega_0\tau = 0$.

midband and at both edges. It has been shown elsewhere[7] that fades matched in this way will be identical in band to within a few tenths of a decibel at most, and will have almost identical envelope delay distortion. Given noisy quantized measurements of $|H(\omega)|$ over the band, it is impossible to distinguish between such fades unless we fix one of the four parameters. Let us consider each of the four possibilities.

2.2 Pseudo two-path fade

If one fixes the amplitude, a, at unity, the simple three-path fade reduces to a two-path fade with independent control of the frequency of the minimum of the response. The difficulty with this model, as may be seen by referring to Fig. 2b, is that it can provide in-band minima only for $|H(\omega)| < 1$ and maxima in-band only for $|H(\omega)| > 1$. In other words, the model cannot match an in-band maximum at an arbitrary fade level. In addition, it was found that during approximately half the periods when the radio equipment was indicating errors, the channel could not be well modeled with a pseudo two-path model.

2.3 Scaled two-path fade

If one fixes the phase, $\phi = \omega_0\tau - \pi$, in the simple three-path model at 0, the fade reduces to a scaled two-path fade. (For a two-path fade, we require the additional condition $a = 1$.) This is the most physically desirable of the reduced three-path models because it may be derived without recourse to the three-path formalism. Unfortunately, it is mathematically intractable, particularly when dealing with amplitude data only. In fitting the model to a given channel shape (in the manner described in Section III for the fixed delay model), one obtains a function of a, b, and τ that must be minimized to obtain the best fit. Because of the $\omega\tau$ term in the exponent of the model, this function has a local minimum in every interval of τ of length 0.17 ns, the reciprocal of 6 GHz. Since the possible range of τ extends to about 30 ns, one may have to perform hundreds of minimizations to find the best fit to a single channel scan. Even then this "best fit" may have no minimum phase realization, and there is no known procedure that leads to one.

2.4 Fixed b model

If one fixes the amplitude b in the simple three-path model, the resulting reduced model has all the mathematical difficulties of the scaled two-path model and no satisfactory physical interpretation.

2.5 Fixed delay model

It is demonstrated in the remainder of this paper that the fixed delay model described in Section I is useful and effective in characterizing the channel.

III. ESTIMATION PROCEDURES

This section describes how the model parameters are estimated from the channel scans and how realizability difficulties are surmounted.

3.1 Parameter estimation

The channel data consist of a set of 25,000 scans of the channel power spectrum. Each scan consists of a power measurement at each of 24 frequencies at 1.1-MHz spacing across the channel. (Actually, only 23 frequencies are used since the 19th was inoperative during this test period). The power measurements are recorded in decibels, and each must be referenced to the average power level of that frequency at mid-day. With proper conversion and calibration, the basic data characterizing a scan are a set of power ratios. We designate the power ratio at nth frequency by Y_n, where

$$Y_n = Y(\omega_n) \qquad n = 1, 2, \cdots, 24. \tag{3}$$

We wish to model the channel with a voltage transfer function of the form given in eq. (1), which we repeat here for convenience

$$H(\omega) = a[1 - be^{\pm j(\omega-\omega_0)\tau}], \tag{1}$$

Thus our estimate of Y_n will be

$$\hat{Y}_n = |H(\omega_n)|^2 = \alpha - \beta \operatorname{Cos}(\omega_n - \omega_0)\tau, \tag{4}$$

where

$$\alpha = a^2(1 + b^2)$$

$$\beta = 2a^2b. \tag{5}$$

For convenience, we measure frequency in the units of the frequency separation of the power measurements. Thus,

$$\omega_n = 2\pi f_n = 2\pi n(1.1 \times 10^6) \quad n = 1, 2, 3, \cdots, 24. \tag{6}$$

If we choose

$$\tau = \frac{1}{N(1.1 \times 10^6)}, \tag{7}$$

then

$$\omega_n\tau = 2\pi \frac{n}{N}. \tag{8}$$

For the fixed delay model, we choose $N = 144$ which gives a model τ of 6.31 ns. Thus, the in-band frequencies correspond to n values between 1 and 24, and the channel transfer function given by the model is periodic for n modulo 144, corresponding to a frequency shift of $144 \times 1.1 \times 10^6 = 158.4$ MHz.

The weighted mean-square error between the estimated and observed power is given by

$$E = \frac{\sum_{n=1}^{24} C_n (Y_n - \hat{Y}_n)^2}{\sum_{n=1}^{24} C_n}, \tag{9}$$

where the summation skips $n = 19$ as described above, and where C_n is a weighting applied to the measurement at frequency ω_n. Since the original data, from which the Y_n's were derived, were uniformly quantized on a logarithmic scale, it is appropriate to use a weighting that is approximately logarithmic. Hence, we use the weighting function

$$C_n = \frac{1}{Y_n^2}. \tag{10}$$

A number of different weighting functions were tested, but the one given by (10) is, generally, the most satisfactory.

Estimates of a, b, and f_o may be obtained by minimizing the weighted mean-square error, E. It is shown in the appendix that one may obtain closed form estimators for α, β, and f_o by substituting eq. (4) into (9) and minimizing E, first with respect to α, then with respect to β (or vice versa), and last with respect to f_o. In the resulting scheme, the estimator of f_o, the frequency of the model minimum, is a function of data only. The estimators of α and β are functions of the estimated f_o and the data.*

After estimates of α and β have been calculated, the parameters a and b of the model are obtained by inverting the relationships given by eq. (5).

$$b = \frac{\alpha}{\beta} - \left[\left(\frac{\alpha}{\beta}\right)^2 - 1\right]^{1/2} \tag{11}$$

$$a = \left[\frac{\beta}{2b}\right]^{1/2}. \tag{12}$$

It is clear from (11) and (12) that we can realize the channel shape with the model only if $\alpha \geq \beta$. This is to be expected. Since $|H(\omega)|^2$ is a power transfer function, it must be positive for all frequencies, which is possible only if $\alpha \geq \beta$ [see eq. (4)]. Thus, the condition $\alpha \geq \beta$ allows us to obtain a minimum (or nonminimum) phase transfer function whose magnitude squared is the minimum weighted mean-square error fit to the observed power transfer response of the channel.

* For mathematical simplicity, we actually use an estimator for β conditioned on f_o, α, and the data.

3.2 Application of estimators

If the procedure described above is strictly applied to the set of 25,000 scans in the data base, one finds that about 35 percent of the scans cannot be modeled with real values of a and b. A study of these problem scans revealed that the estimator for f_o, the frequency of the fade minimum, was biased for two types of scans. One type is a scan with little shape, dominated by quantization noise; the other is a selective channel shape having a steep slope across the band. Both types of scan are illustrated in Fig. 4. The scan in Fig. 4, which is almost flat, was fabricated to illustrate the severity of the quantization problem. The other scan is typical of the more shapely troublesome scans.

To obtain a good realizable fit to such channel shapes requires degrading the quality of the fit; that is, moving the parameters away from the values that minimize the fit error, eq. (9). Given the form of the estimation scheme, this is easily accomplished by moving the frequency of the fade minimum, f_o, away from its original "optimum" value and reoptimizing the remaining parameters to obtain values of a and b that are optimum for the new value of f_o. Figures 5 and 6 illustrate the results of such a quasi-optimization regarding f_o as a free parameter. They show the fit error E and the values of a and b as f_o is varied from its original optimum value. Figure 5 corresponds to the flat fade in Fig. 4 and Fig. 6 to the sloped fade.

The shapes of the curves in Figs. 5 and 6 are typical of those obtained when the channel has no minimum in band. The weighted error in the fit, E, is not very sensitive to the estimate of f_o, the

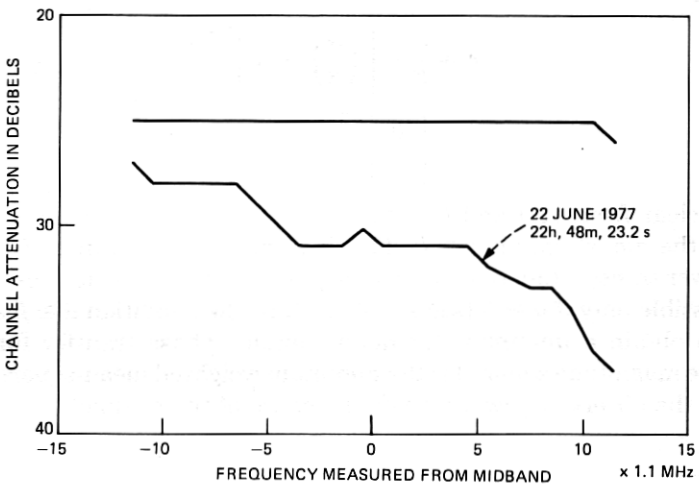

Fig. 4—Two channel scans that produce realization difficulties.

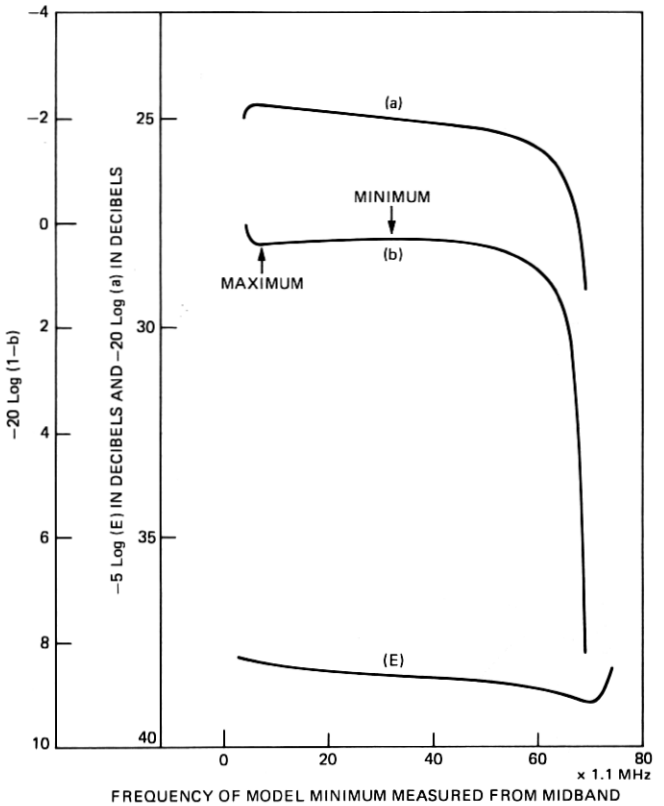

Fig. 5—Locus of weighted fit error and model parameters with f_o as a free variable for flat fade in Fig. 4.

frequency of the modeled fade minimum. The minimum of E is broad and flat, due to quantization and instrumentation noise in the channel. The variation of the parameter a with f_o is also typically very gradual. The salient features of the variation of b with respect to f_o are clearly seen in Fig. 6, and are also present and labeled in Fig. 5. As f_o is varied from its original optimum value, b varies from a value of 1 to a value of 0 in a sideways s-curve with two stationary points, a maximum and a minimum. Extensive simulations with known channel characteristics indicate that a good choice of parameters is the set corresponding to the point where b is locally minimized. To illustrate this point, assume that the channel shape is that given by the model, with 6.3-ns delay, f_o at 18.5 × 1.1 MHz, $a = 0.04$, and $b = 0.7$. One can construct a plot similar to Figs. 5 and 6 for this simulated fade, with the result shown in Fig. 7. The curves in this figure illustrate the results cited above, in that the true value of f_o occurs near a minimum value of b. A better

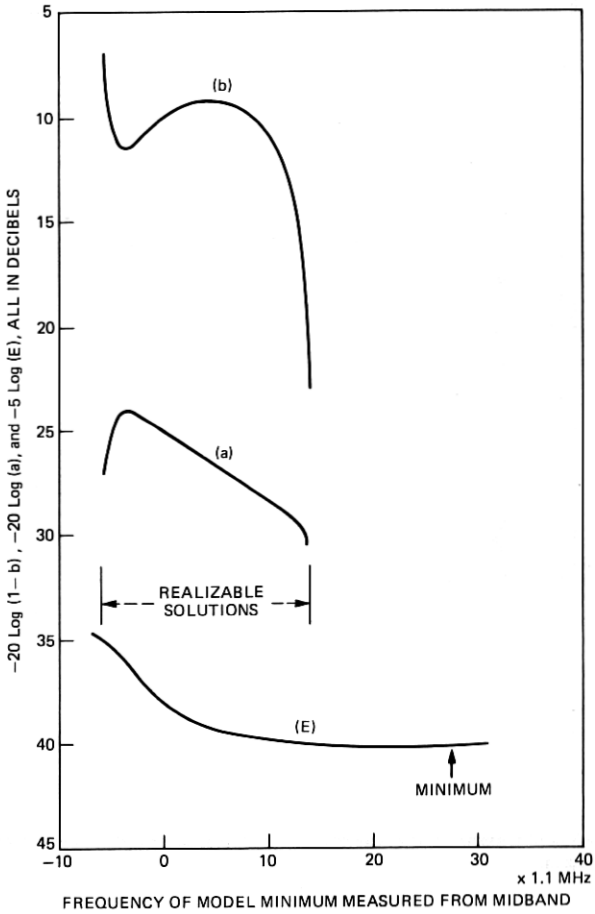

Fig. 6—Locus of weighted fit error and model parameters with f_o as a free variable for typical scan in Fig. 4.

choice for the case shown and for others that have been simulated would be "on the shoulder" between the minimum and $b = 1$; however, such a criterion is difficult to quantify.

To summarize, if the standard routine does not provide a realizable fit to a scan, one merely varies f_o, the position of the minimum, until one obtains a realizable solution with a value of b that is stationary* with respect to variations in f_o. We recognize that this procedure introduces additional sources of error into the estimates of the model parameters. The errors in a and b are small because b is near a stationary value and a is slowly varying. The error in f_o is also small,

* Since b is a monotone function of α/β, it is only necessary to invert solutions with stationary values of the ratio, α/β.

usually less than 3 MHz, but is always in the direction corresponding to moving the minimum nearest to the band closer. We consider the effects of these errors in Section VI.

IV. MODEL STATISTICS

Applying the procedures described in Section III to the scans in the data base results in 25,000 sets of values of a, b, and f_o. The relative joint frequency of occurrence of these three parameters may be described by the set of distribution functions shown in Figs. 8 to 12. The distribution of the parameter b is described in Fig. 8 in terms of the distribution of $-20 \log (1 - b)$, which is approximately exponentially distributed with a mean of 3.8 dB. This distribution gives the time that b exceeds the value given by the abscissa as a fraction of the time in a heavy fading month that the rms level in the channel is depressed by more than 15 dB. For instance, we see that 40 percent of the time

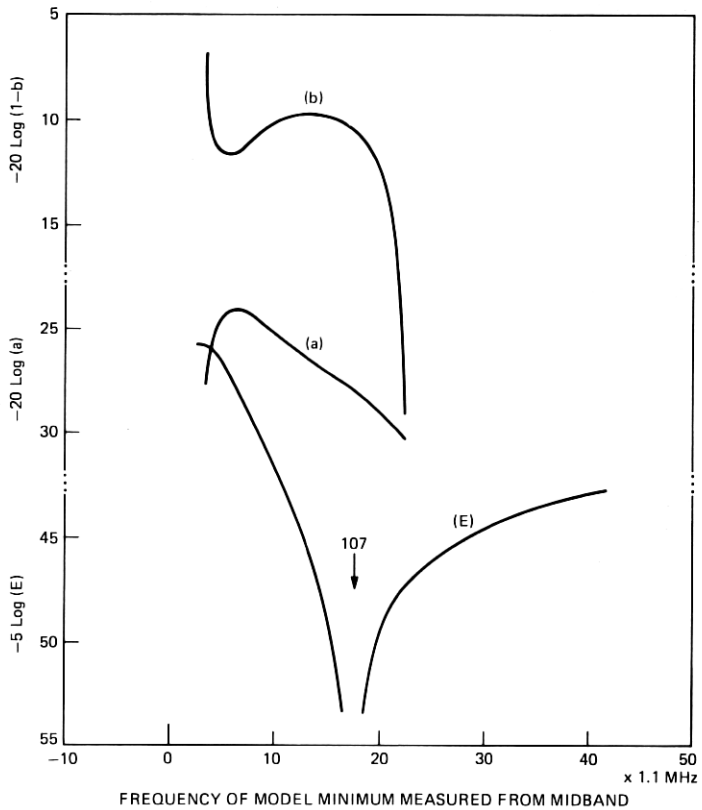

Fig. 7—Locus of weighted fit error and model parameters with f_o as a free variable. For channel given by model with $\tau = 6.31$ ns, $a = 0.04$, $b = 0.7$, $f_o = 18.5 \times 1.1$ MHz.

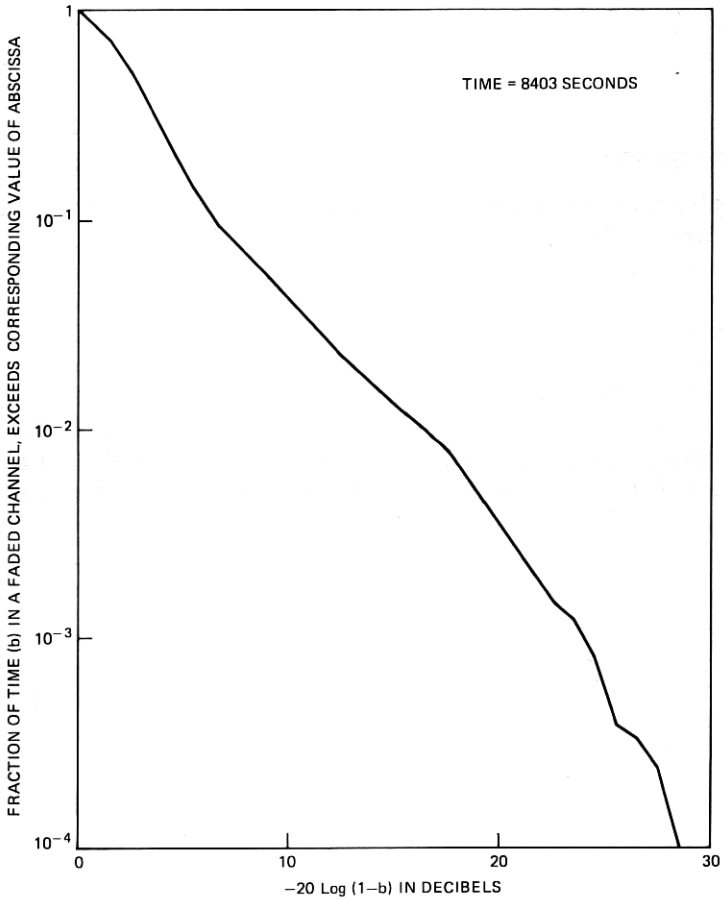

Fig. 8—Distribution of b.

when the channel is depressed the value of b exceeds 0.3. It exceeds 0.7 for 4 percent of that time, and 0.99 about 0.3 percent of that time. The distribution of b can be modeled in the form

$$P(1 - b < X) = X^{\frac{20}{3.8 \text{ Log } 10}} = X^{2.3}. \tag{13}$$

The distribution of a is conditioned on b and is approximately lognormal as shown in Figs. 9 and 10. The mean and standard deviation of the distributions in Figs. 9 and 10 are plotted in Fig. 11. From Figs. 9 to 11 it is apparent that a and b are almost independent; however, less shapely fades tend to occur at less depressed values. We note that shape occurs when the average depression is 20 to 25 dB,* that the

* The value of a corresponds to average power level over a large frequency span and not strictly to the average power in a narrowband channel.

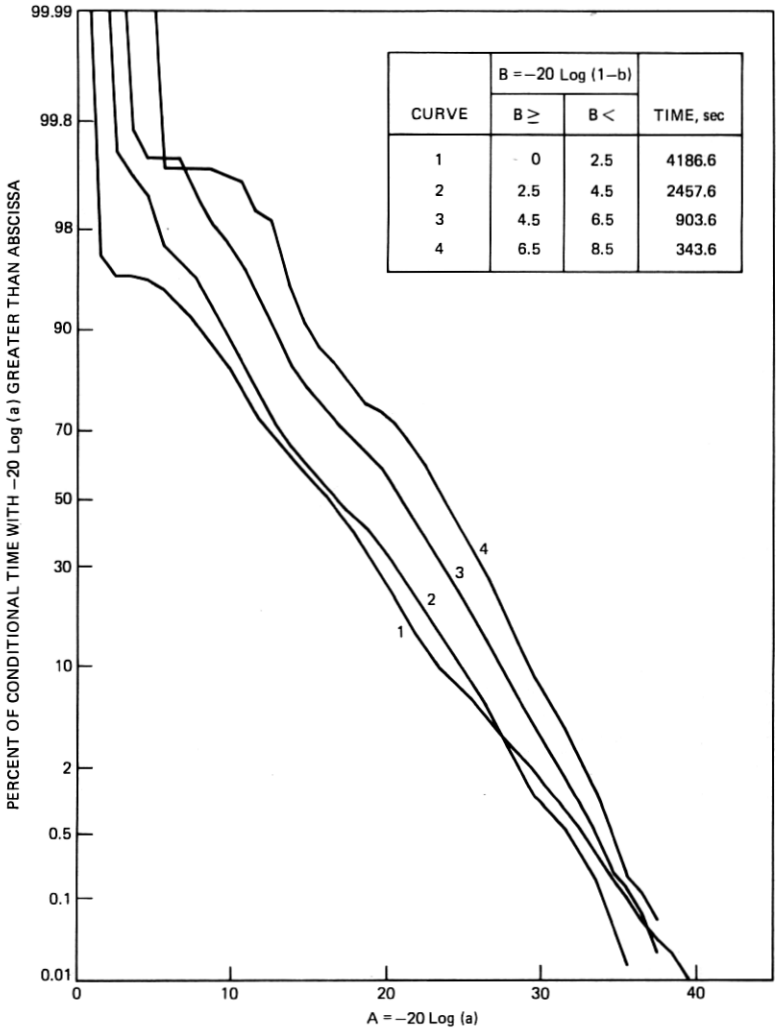

CURVE	B = −20 Log (1−b) B ≥	B <	TIME, sec
1	0	2.5	4186.6
2	2.5	4.5	2457.6
3	4.5	6.5	903.6
4	6.5	8.5	343.6

Fig. 9—Distribution of a conditioned on the value of b for $-20 \log (1 - b)$ less than 8.5 dB.

average depression is near 25 dB for b greater than 0.7, and that it falls off gradually to 15 dB for small b. The distribution of $A = -20 \log a$ is conditioned on b and may be modeled as

$$P(A > Y) = 1 - P\left[\frac{Y - A_o(b)}{5}\right], \tag{14}$$

where P is the cumulative distribution function of a zero mean, unit variance, and Gaussian random variable, and $A_o(b)$ is the mean of A for a given value of b as given in Fig. 11. We see from Fig. 11 that the

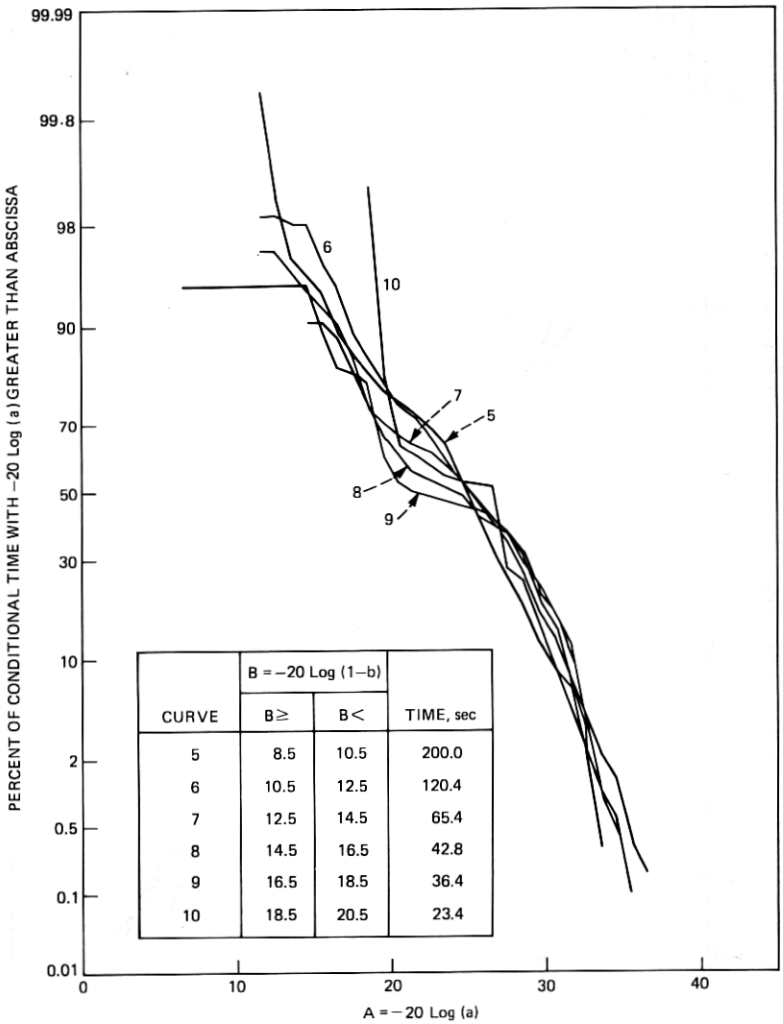

CURVE	B = −20 Log (1−b) B≥	B<	TIME, sec
5	8.5	10.5	200.0
6	10.5	12.5	120.4
7	12.5	14.5	65.4
8	14.5	16.5	42.8
9	16.5	18.5	36.4
10	18.5	20.5	23.4

Fig. 10—Distribution of a conditioned on the value of b for $-20 \log (1 - b)$ greater than 8.5 dB.

standard deviation of A may be taken as 5 dB regardless of the value of b; the variations near $-20 \log (1 - b) = 20$ are due to small sample problems.

Figure 12 shows the time during which scans had f_o in 4×1.1-MHz frequency intervals. It is, in effect, an estimate of the density function of the distribution of f_o and is, consequently, quite noisy. The maxima near $\pm 30 \times 1.1$ MHz from the center of the band are due in part to the movement of estimates of f_o to achieve realizability. While, on physical grounds, one would expect f_o to have a uniform distribution, the fixed

delay model is decidedly not a physical model. Consider a simulated set of simple three-path fades having a uniform distribution of f_o, fixed values for a and b, and a delay τ, fixed at a value other than 6.31 ns. This set of fades will engender a nonflat probability density function for the f_o's obtained in fitting to the 6.31-ns model. The probability density function is flat within the band regardless of the fixed delay of the set of simulated fades; however, it will more nearly resemble that shown in Fig. 12 if the delay of the set is greater than 6.31 ns than if it is less than 6.31 ns. In short, Fig. 12 is characteristic of a channel with a considerable fraction of delay differences greater than 6 ns.

Based on Fig 12, we approximate the probability density function of f_o by a two-level function. Note that f_o is defined on an interval of length $1/\tau$, where τ is 6.3 ns the delay of the model. Thus, with f_o measured from the center of the band, the probability density function for f_o may be approximated by

$$p_{f_o}(f_o) = \begin{cases} \dfrac{5\tau}{3} & |f_o| \leq \dfrac{1}{4\tau} \\ \dfrac{\tau}{3} & \dfrac{1}{4\tau} < |f_o| < \dfrac{1}{2\tau}. \end{cases} \tag{15}$$

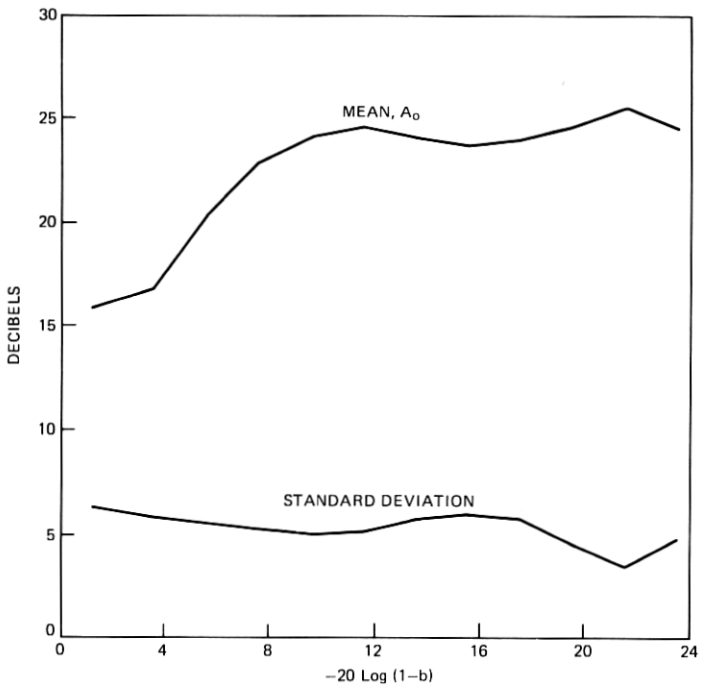

Fig. 11—Mean and standard deviation of the distribution of $-20 \log a$ as a function of $-20 \log (1 - b)$.

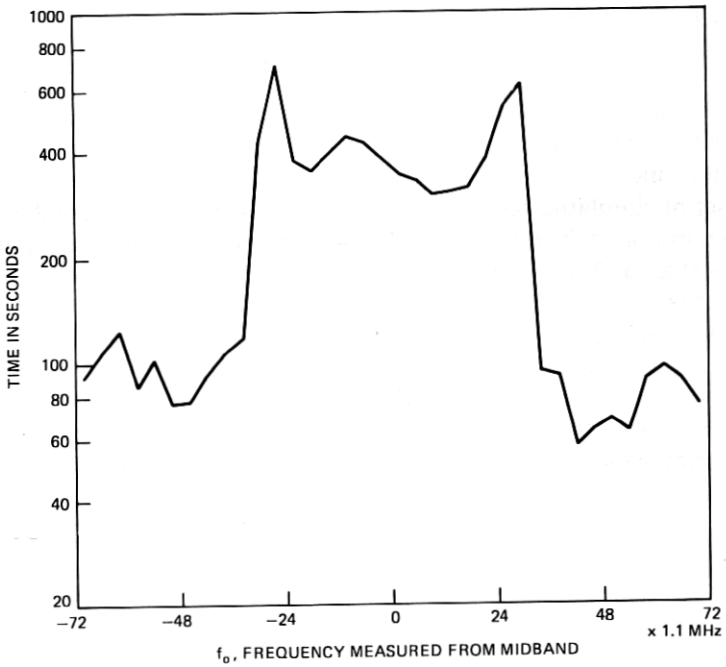

Fig. 12—Time that model parameter, f_o, was in intervals of width 4 × 1.1 MHz.

An extensive examination of various conditional distributions has established that there are no other obvious and pervasive dependencies among the statistics of the parameters.

V. CHANNEL DELAY DIFFERENCE

This section presents some results obtained in estimating the channel delay difference. Some techniques described here are used in the error analysis in Section VI. Three topics are considered in this section. First a simple method is presented of estimating the average delay spread in the channel. A second subsection shows that the distribution of large delays (larger than 10 ns) can be obtained for a simple three-path fade model. The delay distribution is shown to be consistent with the estimate of average delay. A third subsection illustrates the problem with an observed channel shape that can be matched most successfully using a simple three-path model with a delay of approximately 26 ns.

5.1 Mean delay difference in the channel

The mean delay difference of a channel that can be characterized by a simple three-path model is easily estimated. Consider a fade with a delay, τ. If f_o, the frequency of the minimum, is uniformly distributed,

the probability that such a fade produces a minimum in a band B Hz wide is equal to the ratio of the bandwidth to the spacing of the minima, or

$$\frac{B}{1/\tau} = B\tau. \tag{16}$$

If $p(\tau_k)\Delta\tau$ is the fractional number of fades having delays between $(k-1)\Delta\tau$ and $k\Delta\tau$, then the fractional number of fades having a minimum in band will be $P_{\min}$, where

$$P_{\min} = \sum_k B\tau_k p(\tau_k)\Delta\tau = B\bar{\tau} \tag{17}$$

and

$$\bar{\tau} = \sum \tau_k p(\tau_k)\Delta\tau = \int \tau p(\tau)\, d\tau. \tag{18}$$

It follows from eq. (17) that one may estimate the mean delay, $\bar{\tau}$, from a knowledge of $P_{\min}$, the fractional number of scans having a minimum in a band of width B. Since any method of determining $P_{\min}$ is acceptable, consider estimates of $P_{\min}$ from the parameters estimated using the fixed delay model. The method of estimating the frequency parameter in the model involved moving null positions of some fades that had out-of-band minima. These fades can be excluded by using only the central two-thirds of the band in estimating $\bar{\tau}$. Of the 24,920 scans in the data base, 3974 had minima between the $4th$ and $20th$ frequencies. Hence,

$$\bar{\tau} = \left[\frac{3974}{24920}\right] \frac{1}{16 \times 1.1 \times 10^6} = 9.1 \text{ ns}. \tag{19}$$

One might argue that the mean delay should be estimated for a more carefully screened set of scans. Table I shows the mean delay estimates obtained from scan populations qualified by having the estimate of the model parameter a in a given 5-dB interval. Table II

Table I—Mean delay for scans selected by value of parameter, a

$-20 \log a$, dB	Number of Scans	Scans with Min. in Band	Delay, $\bar{\tau}$, ns
0–5	101	31	17.4
5–10	725	235	18.4
10–15	4299	875	11.6
15–20	6891	1161	9.6
20–25	7644	906	6.7
25–30	4184	606	8.2
30–35	1019	159	8.9
All	24920	3974	9.1

Table II—Mean delay for scans selected by value of parameter, b

$-20 \log 1\text{-}b$, dB	Number of Scans	Scans With Min. in Band	Delay, $\bar{\tau}$, ns
0–2	10,442	1186	6.5
2–4	7040	1712	13.8
4–6	3721	538	8.2
6–8	1474	191	7.4
8–10	892	118	7.5
10–12	527	68	7.3
12–14	282	28	5.6
14–16	190	21	6.3
16–18	146	46	17.9
18–20	99	32	18.4
All	24920	3974	9.1

shows mean delay estimates qualified by the model parameter b, which specifies the shapeliness of the fade.

With several exceptions, the estimated delay spreads given in Tables I and II are reasonably constant. One exception is seen for large values of b ($-20 \log 1 - b$ greater than 16). This is consistent with a channel for which large differential attenuation across the channel is more likely to occur when long delays are present. The existence of such a correlation should not be surprising. The other exception is the large delays estimated for small values of b and for values of a between 0 and 10 dB. We provide strong evidence of the existence of such a class of fades in the next subsection. The existence of this subclass of fades suggests that they have a different physical source than the other fades in the population.

5.2 Distribution of delay difference

To further enhance our knowledge of the distribution of delay in the channel, the data base was processed to extract a delay estimate. Recall that, for the fixed delay model, parameter estimates are chosen to minimize the weighted fit error [E in eq. (9)] for a given fixed τ. The present calculation was performed for a set of different values of τ and the value which produced the smallest weighted fit error and corresponded to a realizable fade was designated as the delay for that scan if it met certain qualifications.

Because of the degeneracy in the simple three-path model, changing the delay in the fixed delay model will not appreciably improve the fit for any scan that can be well approximated by a fixed delay of 6 ns or less.[7] In performing the optimum delay calculation, the weighted fit error was minimized for a predetermined set of delays; the differences between adjacent delay values were chosen to be approximately 15 percent. A given scan was assigned a delay different from 6.3 ns only if the third best value of the weighted fit error was at least 0.1 dB worse than the best value. (We use the third best value because we

must examine three values to detect a minimum.) This criterion sets a threshold on the acceptable sharpness of the minimum in the fit error with respect to changes in delay.

The selection criterion was chosen, after several iterations, to insure regularity in the estimates derived from successive scans. With the chosen criterion, the scans that were assigned a new delay occurred in groups of consecutive scans and may be said to constitute fading events. During any of these events, the delay was consistent in that indicated delays were within ±15 percent. If we assume that the physical channel does not change between scans, we can associate a time with each scan and plot the distribution of the time periods during which the characterizing delay was greater than a specified delay.

A series of such plots, conditioned on the concurrently estimated value of b, is given in Fig. 13. The uppermost curve contains the data derived from all scans which met the selection criterion; its shape is

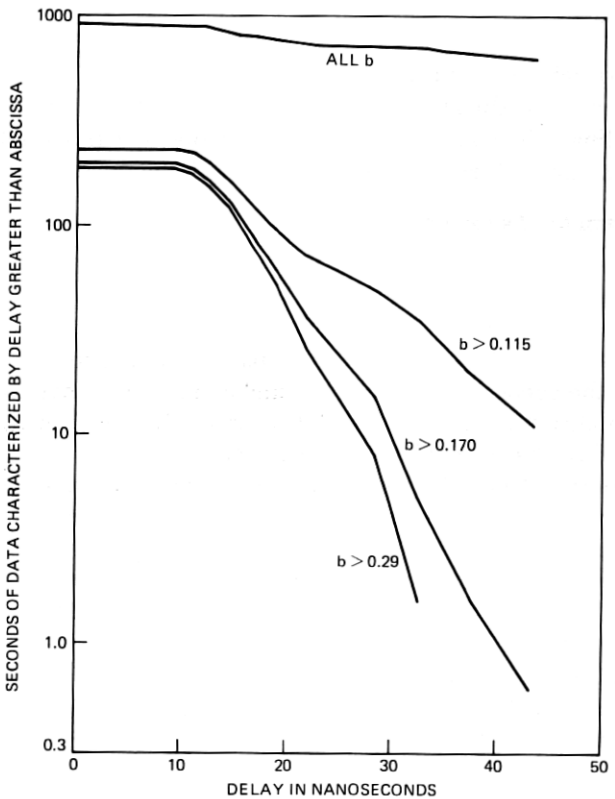

Fig. 13—Distribution of optimum delay for simple three-path model, as qualified by realizability, the sharpness of minimum, and by several values of the model parameter b.

dominated by the 627 seconds during which the channel was best modeled by a delay of 43 ns (the largest delay in the test set) or more, but had little shape ($b < 0.115$). These characteristics contribute to the large (18 ns) mean delays noted in the previous subsection for small values of b. They may be due to quantization but are apparently not artifacts of the estimation scheme. Although the origin of this type of channel defect is currently not understood, it should not trouble any existing radio system.

It is apparent from the distributions in Fig. 13 that very few scans qualified for a new delay with delays less than 10 ns. Consequently, the distribution should not be trusted for delays less than 12 or 15 ns; beyond 15 ns, it may be interpreted as a lower bound to the true distribution. The three curves qualified by the parameter b correspond to fades with peak-to-peak variability of 2, 3, and 6 dB. (Peak-to-peak variability is $20 \log(1 + b/1 - b)$, as may be seen in Fig. 1.) If the delay were exponentially distributed, the distribution of delay would be a straight line on Fig. 13 and would have the form

$$P(\tau > x) = e^{-x/\bar{\tau}}. \tag{20}$$

Fitting a straight line to the three distributions in Fig. 13 for which $b > 0.115$ shows that the average delay decreases with increasing b. The corresponding values are 5, 5.5, and 11 ns. Note that this implies that b and τ in a simple three-path model are not independent.

5.3 An example of a long delay scan

To confirm the existence of long delay scans, consider an event that covered approximately 10 seconds on 22 June 1977, from 23 h, 28 m, 54 s. A representative scan from the middle of this period is shown with the fit obtained with the fixed delay (6.3 ns) model in Fig. 14a. To emphasize the consistency of this channel condition, an average of the channel condition for the central 4.2 seconds (21 scans) of this event is compared to the selected scan in Fig. 14b.

It is apparent from Fig. 14*a* that the 6.3 ns delay does not have enough curvature (delay is too short) to precisely model the channel shape. Figure 15 shows the same scan modeled by three-path fades having delays of 22.7, 26, and 30.3 ns. The 26-ns fit is the best; it has a weighted fit error 0.4 dB better than the 22.7-ns fit and 0.8 dB better than the 30.3 ns fit. However, the closeness of all three fits illustrates the difficulties in estimating channel delay differences. Visually, one would choose the 26-ns model on the basis that the 30.3-ns fit has too much curvature and the 22.7-ns fit too little.

VI. ERROR ANALYSIS

To verify that the model adequately represents the transmission characteristics of the channel, we examine the errors between the

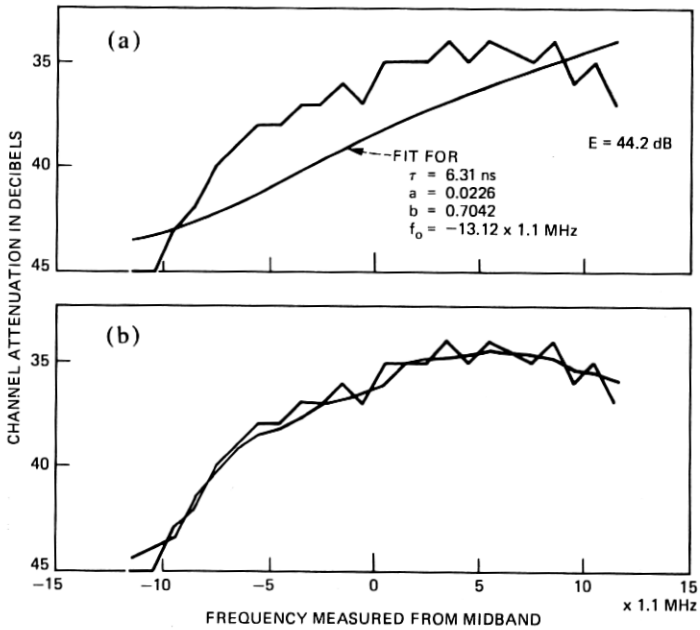

Fig. 14—Scan from 22 June 1977, 23 h, 28 m, 48.6 s. (a) Comparison with fixed delay model. (b) Comparison with average of scans from 23 h, 28 m, 46.4 s to 23 h, 28 m, 50.4 s.

channel as observed and as modeled. In this section we consider the statistics of the rms errors and the maximum errors.

6.1 RMS errors

A useful measure of the quality of the fit of the model to a given channel scan is the root-mean-square value of the decibel error at each of the sampled frequencies. Denoting this error as E_{rms}, we have

$$E_{rms} = \left[\frac{1}{23} \sum_{\substack{n=1 \\ n \neq 19}}^{24} (\text{dB error at } f_n)^2 \right]^{1/2}. \tag{21}$$

The model parameters were estimated, as described in Section III, to minimize the error, E, which is a weighted sum of the squares of the power differences at each frequency [see eq. (9)]. The weighting was chosen [eq. (10)] so that the error E would approximate the error E_{rms} as given by eq. (21).* Indeed, one may show directly that the two expressions are equivalent as long as

$$\left| 1 - \frac{\hat{Y}_n}{Y_n} \right| \ll 1 \text{ for all } n. \tag{22}$$

* Note that the parameter estimation problem cannot be solved in closed form by minimizing E_{rms}.

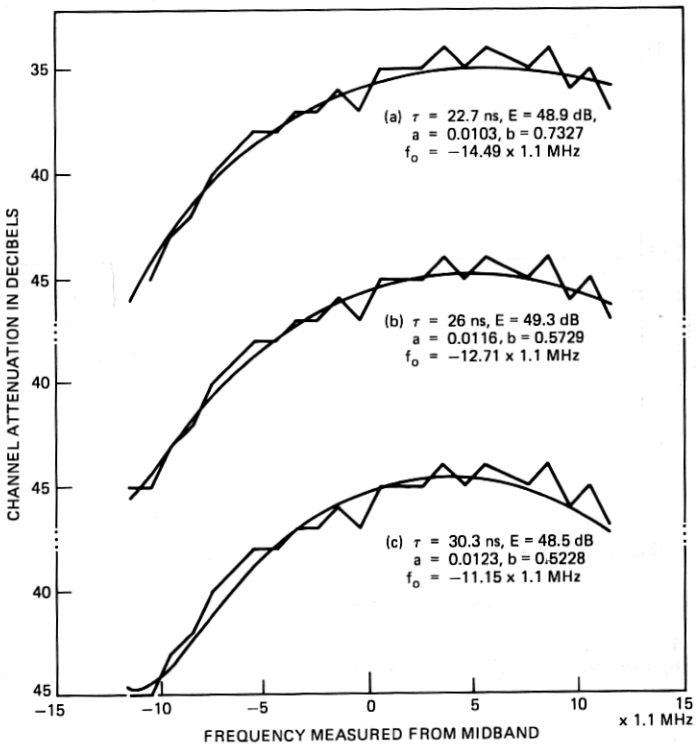

Fig. 15—Model fits to long delay scan for three different model delays.

As we have seen in Fig. 14, this inequality is not always satisfied. Consequently, in using E_{rms} as a standard of comparison, we are evaluating not only how well the model fits the observed channel, but also how well we have chosen the parameters to make the match.

The error E_{rms} is a desirable quantity to work with because we can estimate its distribution under the assumption of perfect matching. We observe that if the decibel error were Gaussian with unit variance and zero mean, $23\ E_{rms}^2$ would be a χ^2 variable with 20 degrees of freedom (to account for the three parameters estimated per scan). Observations of a simulated channel with the transmitter and receiver back-to-back indicate that the instrumentation errors are approximately Gaussian with a standard deviation, σ_i, of about 0.65 dB. Observations of the channel at mid-day with the channel nominally flat and unfaded indicate that the standard deviation of the errors is between 0.68 and 0.73, varying frequency to frequency and day to day by a few hundredths of a decibel. Hence, if we enter a table of the χ^2 distribution, $Q(\chi^2 \mid 20)$, with

$$\chi^2 = \frac{23\ E_{rms}^2}{\sigma_i^2}, \tag{23}$$

we can determine the distribution of E_{rms} under the assumption of perfect matching.* This distribution is shown as a reference on Figs. 16 and 17. It is indicated by a solid curve labeled "ideal" for $\sigma_i = 0.70$ and by o's for $\sigma_i = 0.75$.

Figure 16 presents the distribution of the rms error for two scan subpopulations using the fixed delay (6.3 ns) model. The subpopulation of the distribution labeled "standard" consists of all scans that could be modeled directly; the distribution labeled "modified" shows the rms error distribution for all scans which required an adjustment of the frequency of the modeled fade to achieve realizability. Figure 17 shows the distribution of the rms error for the composite of all samples using the fixed delay (6.3 ns) model. The distribution labeled simple three-path model indicates the error distribution that was obtained when the scan fitting allowed unqualified variation in model delay to achieve the best fit. That is, the calculation described in Section 5.2 was performed and the results were qualified only on the basis of realizability.†

In each case described above, the mean value of the rms error is close to the median value. For the two subpopulations shown in Fig. 16, the calculated mean fit errors correspond to σ_i values of 0.76 and 0.85 dB, or the errors are about 0.09 dB larger when a realizable fit is obtained by varying the frequency of the model minimum. Comparing the composite distributions in Fig. 17, we find that the mean error in the fixed delay (6.3 ns) model corresponds to $\sigma_i = 0.78$ dB or about 0.08 dB higher than that observed when the channel is quiescent. The simple three-path model has a distribution of rms error that very nearly matches the ideal distribution (with 19 degrees of freedom) for $\sigma_i = 0.75$. This is consistent with the instrumentation error imputed to the standard distribution in Fig. 16 and is indicative of the instrumentation error in the presence of multipath fading. It is exceptionally good considering that the data are obtained from time sequential measurements on a dynamically changing channel. One concludes that the modeling error is negligible for the simple three-path model. For the fixed delay model under the assumption that the instrumentation and modeling errors add in quadrature, the modeling error has a tolerable value on the order of 0.2 dB. That is,

$$[(0.75)^2 + (0.2)^2]^{1/2} = 0.776.$$

The tails of the distributions in Figs. 16 and 17 for large errors are of considerable interest. The tails near small values are of little

---

* From the central limit theorem, we know that E^2_{rms} will be approximately Gaussian, as is χ^2, regardless of whether or not the measurement errors are precisely Gaussian.

† Note that although one cannot always reliably localize the values of the parameters in fitting with the simple three-path model (see discussions in Section 2.1 and Ref. 7), the error in the fit is always well defined.

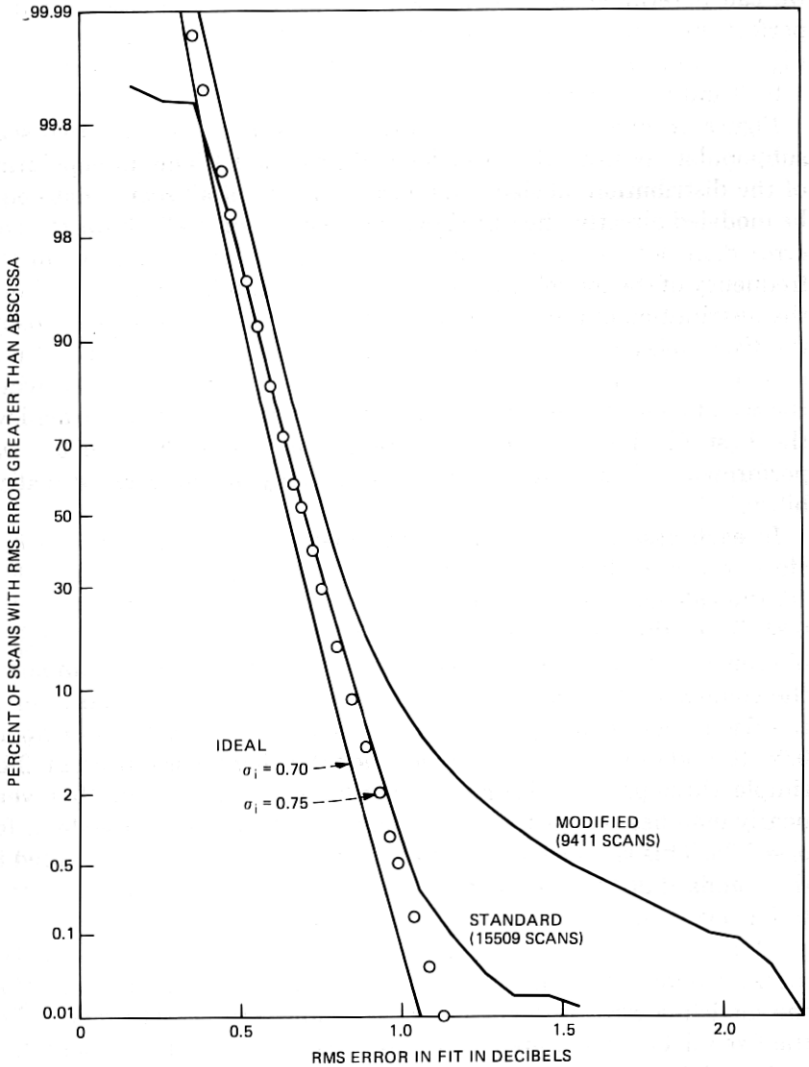

Fig. 16—Distribution of rms fit error for two scan subpopulations with fixed delay (6.3 ns) model.

consequence; they are distorted by quantization because one cannot associate any error with the 12 flat fades included in the data base. The deviation of the distributions from the ideal distribution at large errors is significant.

The large deviation of the modified fits in Fig. 16 reflects the failure of the fixed delay (6.3 ns) model to accurately fit the long delay fades. The tail deviation from ideal is modest down to about the 0.5 percent level, corresponding to a few tens of seconds per month. For compar-

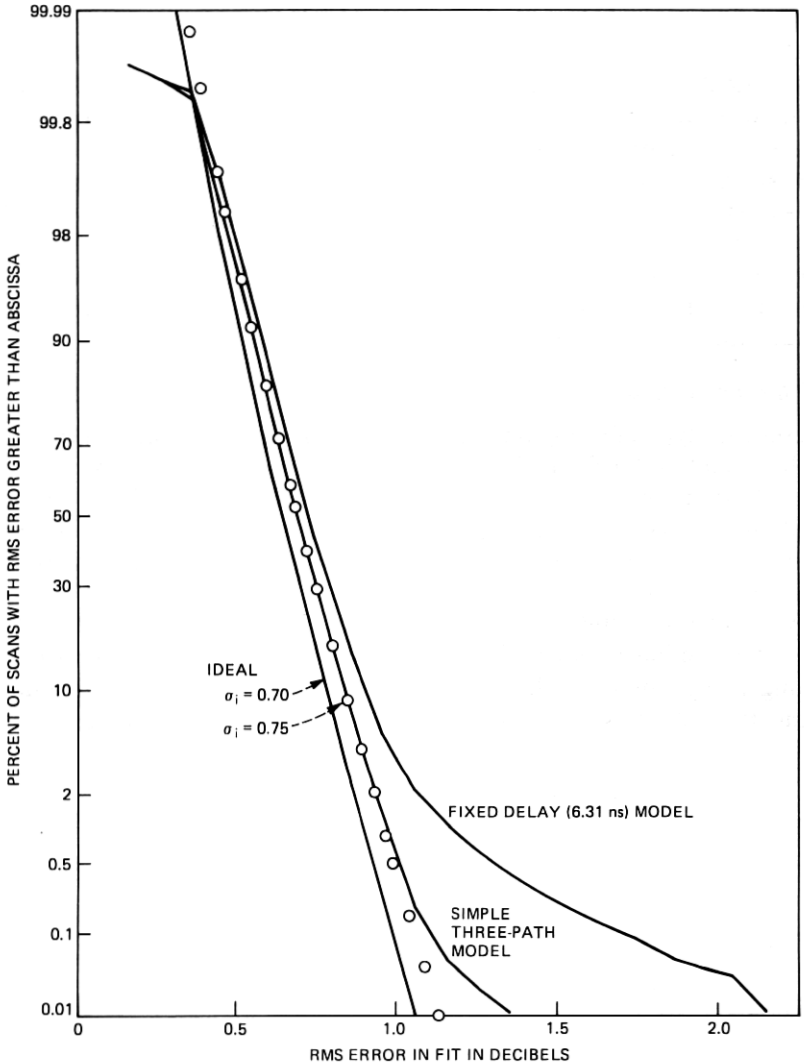

Fig. 17—Distribution of rms fit error for composite population with fixed delay and simple three-path models.

ison, we note that the rms error of the fit shown in Fig. 14a is 2.3 dB; this was the worst fit encountered for the fixed delay (6.3 ns) model. However, even in this case the model failure is hardly describable as severe. The model of the channel is depressed by 40 dB and has 9.5 dB of gain slope; the actual channel is depressed by 39 dB and has 11 dB of gain slope. Also, we note that the 6.3-ns delay model has the response minimum at about the same frequency as the best representation, the 26-ns delay model shown in Fig. 15.

The deviation of the tail of the error distribution for the three-path fade (Fig. 17) reflects the fact that there are fades that even this model has difficulty in fitting. An example of such a fade is shown in Fig. 18 along with the fit provided by the fixed delay (6.3 ns) model. The same rms error (1.6 dB) is obtained for all values of model delay between 0.05 and 9 ns; the fit degrades for larger delays. Either more than three rays are needed to describe the channel shape in Fig. 18, or the channel is so depressed that the amplitudes in the notch are distorted due to closeness to the noise level in the measuring equipment. The scan shown in Fig. 18 is one of three similar scans and has little statistical significance.

6.2 Maximum errors

Another type of error that can be used to judge the quality of the fit of the model to the channel is the worst-case error. That is, after fitting to each scan, one records the magnitude of the largest difference (in decibels) between the observed channel shape and the shape calculated from the model. The following paragraphs consider the distribution of these worst-case errors.

As in the preceding subsection, we can calculate an ideal distribution; however, the ideal distribution is not as realistic in this case since it is strongly dependent on the tails of the distributions of the individual measurement errors. We assume that each power measurement had

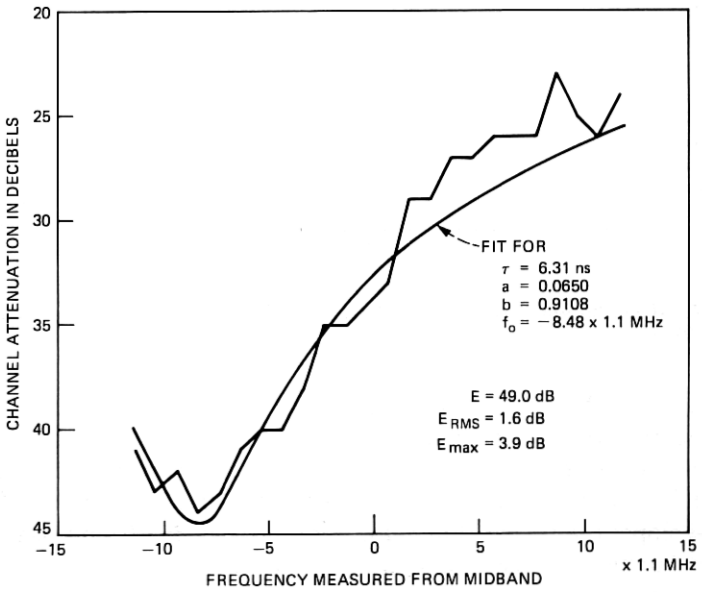

Fig. 18—Severe fade observed on 22 June 1977 at 22 h, 29 m, 8.6 s.

an error in decibels that was Gaussian, with zero mean, a standard deviation of $\sqrt{20/23}\ \sigma_i$ to account for the three parameters estimated from the 23 observations per scan,* and that the errors are independent frequency to frequency. If the probability of any one measurement having an error less than x is denoted by $P_1(x)$, the probability that all 23 have values less than x is

$$P_{23}(x) = [P_1(x)]^{23}. \tag{24}$$

This is the probability that the maximum error is less than x, whereas we want the probability that it is greater than x which we denote $Q_{23}(x)$. It follows immediately from eq. (24) that

$$\begin{aligned} Q_{23}(x) &= 1 - [P_1(x)]^{23} \\ &= 1 - [1 - Q_1(x)]^{23}. \end{aligned} \tag{25}$$

The distribution given by (25) is used as a reference in Figs. 19 and 20, which show the distribution of the maximum error for the same cases as in Figs. 16 and 17. Since the tails of these distributions are well behaved for larger errors, the distribution of the maximum errors is apparently dominated by the instrumentation noise. That is, if we use for the standard deviation of the measurement noise the value obtained from the mean of E_{rms} for one of these cases (as given in Section 6.1), the resulting worst-case error distribution calculated with eq. (25) will closely match the observed maximum error distribution.

VII. CONCLUSIONS

By analyzing the errors in fitting the observed channel characteristics in Section VI, we demonstrated that the simple three-path fade model is indistinguishable from a perfect model of a line-of-sight microwave radio channel.

The simple three-path model was used in Section V to characterize the channel delay difference. By two different methods, it was shown that, when there is 3 dB or more shape present in the channel, the average delay difference is between 5 and 8 ns. We developed a lower bound on the tails of the distribution of delay difference. From these results, which are shown in Fig. 13, we observe that a differential channel attenuation in-band of 3 dB or more may be due to delay differences as great as 43 ns. In another dimension, one would expect to see differential attenuation of 3 dB or more in-band due to delays greater than 20 ns for at least 70 seconds in a heavy fading month. This is comparable to the time the channel attenuation at a single frequency exceeds 40 dB.

---

* For comparisons with the three-path model, it is appropriate to use $\sqrt{19/23}\,\sigma_i$.

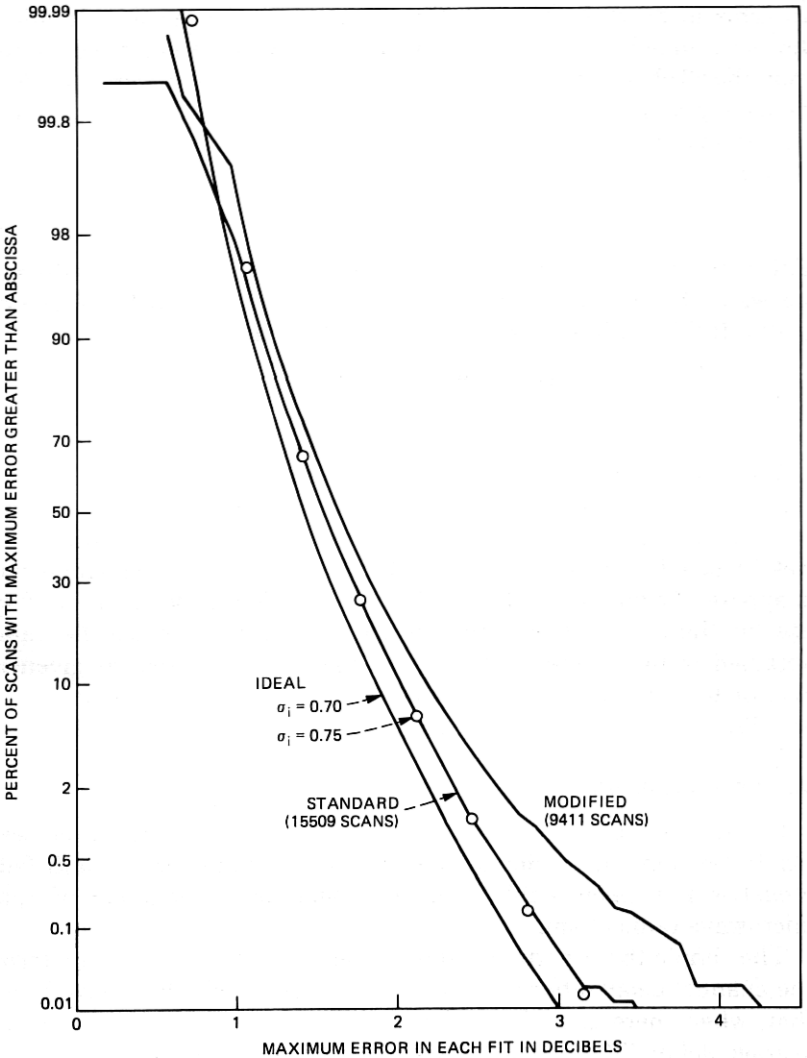

Fig. 19—Distribution of maximum (dB) fit error for two scan subpopulations with fixed delay (6.3 ns) model.

From the error analysis in Section VI, we also conclude that the fixed delay (6.3 ns) model is a very good approximation to the channel for all observed conditions. This conclusion is further substantiated by Figs. 14 and 18, which show the scans for which the fits with the fixed delay model exhibited the largest rms fit error (2.3 dB) and the largest maximum error (3.9 dB), respectively. The fixed delay model is preferable to the three-path model for channel modeling because it requires

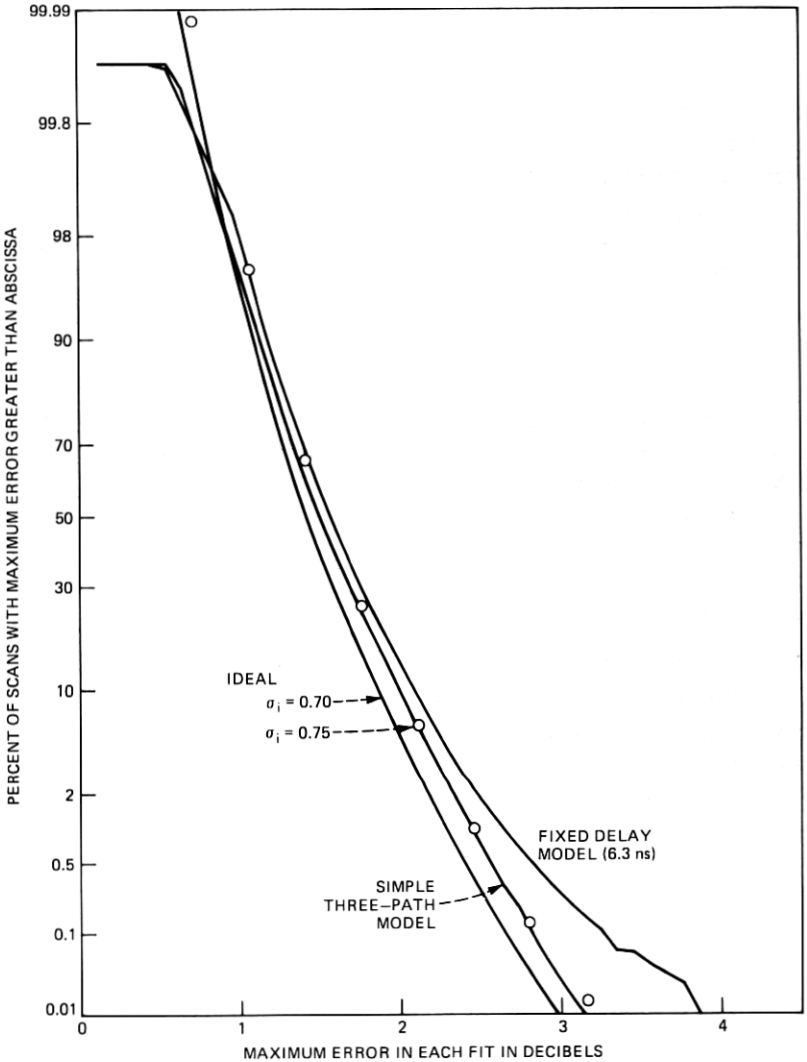

Fig. 20—Distribution of maximum (dB) fit error for composite population with fixed delay and simple three-path models.

only three parameters, and these can always be uniquely determined from a channel amplitude scan.

The statistics of the parameters of the fixed delay model as described in Section IV and shown in Figs. 8 to 12 provide the means of statistically generating all the channel conditions that one expects to see on a nominal hop channel operated at 6 GHz. If one determines, by laboratory test, the parameter values that will cause a particular

error rate in a digital radio system, one can easily calculate the time during a heavy fading month that the error rate will equal or exceed this critical value. A companion paper describes the laboratory test and the required calculations.[8]

Future work will be directed toward verifying the model and model statistics with additional fading data obtained both at 6 GHz and at 4 GHz. Using coherent data obtained in 1973, it will be possible to determine the extent to which the channel is actually a minimum phase channel.

VIII. ACKNOWLEDGMENTS

This study would not have been possible without the contributions of many individuals. In particular, the radio equipment was installed, aligned, and maintained by R. A. Hohmann, C. W. Lundgren, and L. J. Morris with instrumentation designed by G. A. Zimmerman. The data processing expertise in setting up and calibrating the data base was provided by M. V. Pursley.

APPENDIX

Estimation of Parameters

The problem of estimating the parameters α, β, and f_o in Section III is equivalent to the problem of determining the first three terms in a subharmonic Fourier series expansion of a function in the frequency domain. Since such expansions are not standard, we provide a complete description of the methodology here.

From eqs. (4) and (9), we may express the weighted mean-square error between estimated and observed power as*

$$E = \frac{\sum C_n(Y_n - \alpha + \beta \cos(\omega_n - \omega_0)\tau)^2}{\sum C_n}. \tag{26}$$

For simplicity, we use a normalized weighting function, d_n, defined by

$$d_n = \frac{C_n}{\sum C_n} \tag{27}$$

so that

$$\sum d_n = 1. \tag{28}$$

In terms of the normalized weighting we may write (26) as

$$E = \sum d_n(Y_n - \alpha + \beta \cos(\omega_n - \omega_0)\tau)^2 \tag{29}$$

* Throughout this appendix, all summations are taken over all values of n corresponding to all frequencies observed in a scan.

or in expanded form as

$$E = \sum d_n Y_n^2 + \alpha^2 + \beta^2 \sum d_n \cos^2(\omega_n - \omega_0)\tau + 2\beta \sum d_n Y_n \cos(\omega_n - \omega_0)\tau - 2\alpha\beta \sum d_n \cos(\omega_n - \omega_0)\tau - 2\alpha \sum d_n Y_n . \quad (30)$$

The error E is a minimum when α, β, and ω_0 are chosen so that the partial derivatives of E with respect to α, β, and ω_0 are all equal to zero. Setting the partial derivative of eq. (30) with respect to β equal to zero and solving for β gives

$$\beta = \frac{\alpha \sum d_n \cos(\omega_n - \omega_0)\tau - \sum d_n Y_n \cos(\omega_n - \omega_0)\tau}{\sum d_n \cos^2(\omega_n - \omega_0)\tau} . \quad (31)$$

Substituting (31) into eq. (30), we find E_β, the error minimized with respect to β, as

$$E_\beta = \sum d_n^2 Y_n^2 + \frac{1}{\sum d_n \cos^2(\omega_n - \omega_0)\tau} \cdot \{\alpha^2[\sum d_n \cos^2(\omega_n - \omega_0)\tau - (\sum d_n \cos(\omega_n - \omega_0)\tau)^2] - 2\alpha [(\sum d_n Y_n)(\sum d_n \cos^2(\omega_n - \omega_0)\tau) - (\sum d_n \cos(\omega_n - \omega_0)\tau)(\sum d_n Y_n \cos(\omega_n - \omega_0)\tau)] - (\sum d_n Y_n \cos(\omega_n - \omega_0)\tau)^2\} . \quad (32)$$

Minimizing this with respect to α requires that we set the partial derivative of E_β with respect to α equal to zero. This gives

$$\alpha = \frac{(\sum d_n Y_n)(\sum d_n \cos^2(\omega_n - \omega_0)\tau) - (\sum d_n \cos(\omega_n - \omega_0)\tau)(\sum d_n Y_n \cos(\omega_n - \omega_0)\tau)}{\sum d_n \cos^2(\omega_n - \omega_0)\tau - (\sum d_n \cos(\omega_n - \omega_0)\tau)^2} . \quad (33)$$

Substituting (33) into (32) gives $E_{\alpha\beta}$, the error minimized with respect to both α and β, as

$$E_{\beta\alpha} = \sum d_n Y_n^2 - \bar{Y}^2 - \frac{(\sum d_n (Y_n - \bar{Y}) \cos(\omega_n - \omega_0)\tau)^2}{\sum d_n \cos^2(\omega_n - \omega_0)\tau - (\sum d_n \cos(\omega_n - \omega_0)\tau)^2} , \quad (34)$$

where

$$\bar{Y} = \sum d_n Y_n . \quad (35)$$

We note that we could have obtained this same expression by first minimizing with respect to α and then with respect to β; however, one obtains different but equivalent expressions for α and β, depending on

the order of differentiation. We develop the alternative expressions for α and β in the following paragraphs.

Let us define some new quantities to simplify these expressions. Let the difference between the observed power and the weighted mean power in the band be designated by X_n; then

$$X_n = Y_n - \sum d_n Y_n = Y_n - \bar{Y}. \tag{36}$$

If we also define the quantities

$$X_c = \sum d_n X_n \cos \omega_n \tau, \tag{37}$$

$$X_s = \sum d_n X_n \sin \omega_n \tau, \tag{38}$$

$$D_a = \sum d_n \cos^2(\omega_n - \omega_0)\tau, \tag{39}$$

$$D_b = \sum d_n \cos(\omega_n - \omega_0)\tau, \tag{40}$$

we may rewrite α and β from eqs. (31) and (33) as

$$\alpha = \bar{Y} - \frac{[X_c \cos \omega_0 \tau + X_s \sin \omega_0 \tau] D_b}{D_a - D_b^2} \tag{41}$$

and

$$\beta = \frac{1}{D_a} \{(\alpha - \bar{Y}) D_b - (X_c \cos \omega_0 \tau + X_s \sin \omega_0 \tau)\}. \tag{42}$$

Using (41) to eliminate α from (42), we obtain

$$\beta = - \frac{X_c \cos \omega_0 \tau + X_s \sin \omega_0 \tau}{D_a - D_b^2}. \tag{43}$$

We may use (43) in (41) to obtain

$$\alpha = \bar{Y} + \beta D_b. \tag{44}$$

Equations (43) and (44) are the estimators that would have been obtained if the order of taking partial derivatives in the preceding development had been reversed. It is apparent that, after one has estimated ω_0, one may estimate α and β by using either eqs. (41) and (42), (43) and (44), or eqs. (41) and (43).

The estimate of ω_0 that minimizes the weighted error is obtained by minimizing $E_{\beta\alpha}$ with respect to ω_0. Using eqs. (35) to (40) in eq. (34), we write

$$E_{\beta\alpha} = \sum d_n X_n^2 - \frac{[X_c \cos \omega_0 \tau + X_s \sin \omega_0 \tau]^2}{D_a - D_b^2}. \tag{45}$$

To see the explicit dependence of $E_{\beta\alpha}$ on ω_0, we define the following quantities

$$d_c = \sum d_n \cos^2 \omega_n \tau - (\sum d_n \cos \omega_n \tau)^2, \tag{46}$$

$$d_s = \sum d_n \sin^2 \omega_n \tau - (\sum d_n \sin \omega_n \tau)^2, \tag{47}$$

$$d_{cs} = \sum d_n \cos \omega_n \tau \sin \omega_n \tau - (\sum d_n \cos \omega_n \tau)(\sum d_n \sin \omega_n \tau). \tag{48}$$

Substituting these into (45) gives

$$E_{\beta\alpha} = \sum d_n X_n^2 - \frac{[X_c \cos \omega_n \tau + X_s \sin \omega_0 \tau]^2}{d_c \cos^2 \omega_0 \tau + 2 d_{cs} \cos \omega_0 \tau \sin \omega_0 \tau + d_s \sin^2 \omega_0 \tau}. \tag{49}$$

Setting the partial derivative of $E_{\beta\alpha}$, as given by (49), equal to zero gives the estimator for ω_0 as

$$\omega_0 \tau = \mathrm{Tan}^{-1}\left[\frac{d_c X_s - d_{cs} X_c}{d_s X_c - d_{cs} X_s}\right]. \tag{50}$$

Obviously, two values of $\omega_0 \tau$ in the interval $(-\pi, \pi]$ will satisfy eq. (50). One of these, the principal value, lies in the interval $(-\pi/2, \pi/2]$, the other differs from the first by $\pm\pi$. We shall show that the two solutions are equivalent, but that our chosen solution is unique.

If we replace $\omega_0 \tau$ by $\omega_0 \tau \pm \pi$ in eqs. (39), (40), (43), (44), and (45), we see that D_b and β change sign and α and $E_{\beta\alpha}$ are unchanged. Since we want the solution with β greater than zero, we take the principal value solution to (50) if the resulting estimate of β is positive. Otherwise we add or subtract π to obtain a positive value for β and a value of $\omega_0 \tau$ in the appropriate interval.

While we could substitute the result of eq. (50) into (49) to obtain the minimum error, $E_{\alpha B \omega_0}$, it is more generally useful to evaluate $E_{\alpha\beta}$ for the optimum ω_0. This is especially true when we do not use the optimum ω_0, as given by eq. (50). The simplest form for $E_{\alpha\beta}$ is obtained by substituting (43) into (45) to give

$$E_{\alpha\beta} = \sum d_n X_n^2 - (D_a - D_b^2)\beta^2. \tag{51}$$

These equations were implemented, with the modifications described in Section 3.2, to obtain all the fits described in this paper.

REFERENCES

1. G. M. Babler, "A Study of Frequency Selective Fading for a Microwave Line-of-Sight Narrowband Radio Channel," B.S.T.J., *51*, No. 3 (March 1972), pp. 731–757.
2. G. M. Babler, "Selectively Faded Nondiversity and Space Diversity Narrowband Microwave Radio Channels," B.S.T.J., *52*, No. 2 (February 1973), pp. 239–261.
3. L. J. Greenstein, "A Multipath Fading Channel Model for Terrestrial Digital Radio," IEEE Trans. Commun. Tech., *COM-26*, No. 8 (August 1978), pp. 1247–1250.
4. R. L. Kaylor, "A Statistical Study of Selective Fading of Super-High Frequency Radio Signals," B.S.T.J., *32*, No. 5 (September 1953), pp. 1187–1202.
5. G. M. Babler, unpublished work.
6. W. C. Jakes, Jr., "An Approximate Method to Estimate An Upper Bound on the Effect of Multipath Delay Distortion on Digital Transmission," ICC '78 Conference Record, June 1978, *3*, pp. 47.1.1–5.
7. W. D. Rummler, "A Multipath Channel Model for Line-of-Sight Digital Radio Systems," ICC '78 Conference Record, June 1978, *3*, pp. 47.5.1–4.
8. C. W. Lundgren and W. D. Rummler, "Digital Radio Outage Due to Selective Fading—Observation vs Prediction from Laboratory Simulation," B.S.T.J., this issue, pp. 1073–1100.